

Transition-State Alkylation Geometries of 7,8-Dihydroxy-9,10-epoxy-7,8,9,10-tetrahydrobenzo[a]pyrene Enantiomeric Isomers with Nucleic Acid Dimers

O. KIKUCHI *[§], R. PEARLSTEIN *, A. J. HOPFINGER *[¶], and D. R. BICKERS †

Received June 18, 1981, from the *Department of Macromolecular Science, Case Institute of Technology and the †Department of Dermatology, School of Medicine, Case Western Reserve University, Cleveland, OH 44106. Accepted for publication June 25, 1982. ‡Permanent address: Department of Chemistry, The University of Tsukuba, Sakura-mura, Ibaraki, 305 Japan. ¶Alternate address: Department of Drug Design, G. D. Searle and Co., Chicago, IL 60080.

Abstract □ The steric contact spaces associated with the reaction of the enantiomeric isomers of 7,8-dihydroxy-9,10-epoxy-7,8,9,10-tetrahydrobenzo[a]pyrene (I) with the exocyclic amino group of guanine of dinucleoside dimer structures were examined for a fixed transition-state geometry. This reaction is sterically prohibited for the B form DNA conformation. If, however, the nucleic acid structure is deformed, such that the distance between two adjacent base pairs (one containing guanine and cytosine) is maximized, sterically allowed transition-state geometries can be identified. It was not possible to uniquely identify the preferred transition-state complex with respect to nucleic acid structure or isomer of I. However, two types of general transition-state geometries were observed. In one, I was located "outside" the nucleic acid structure; in the other geometry, I was intercalated between adjacent base pairs in the transition state. The intercalation process might serve as a physical catalyst for the alkylation of NH₂-guanine by I.

Keyphrases □ 7,8-Dihydroxy-9,10-epoxy-7,8,9,10-tetrahydrobenzo[a]pyrene—enantiomeric isomers, alkylation of dinucleoside dimers, transition-state geometry □ Dinucleoside dimers—alkylation by enantiomeric isomers of 7,8-dihydroxy-9,10-epoxy-7,8,9,10-tetrahydrobenzo[a]pyrene, transition-state geometry □ Transition-state geometry—of the alkylation of dinucleoside dimers by enantiomeric isomers of 7,8-dihydroxy-9,10-epoxy-7,8,9,10-tetrahydrobenzo[a]pyrene, intercalation

The chemical carcinogen benzo[a]pyrene (II) is metabolized to a diol-epoxide derivative (I) which is enzymatically formed in two stereoisomeric forms: 7β,8α-dihydroxy-9α,10α-epoxy-7,8,9,10-tetrahydrobenzo[a]pyrene [III, designated *anti* or *trans*(eq,eq')] and 7β,8α-dihydroxy-9β,10β-epoxy-7,8,9,10-tetrahydrobenzo[a]pyrene [IV, designated *syn* or *cis*(ax,ax')] (1-6). Each has a complement, *trans*(ax,ax') and *cis*(eq,eq'), respectively, and each of these four isomers can exist as a (+) or (-) enantiomer. The eight possible enantiomeric isomers are shown in Fig. 1, described in terms of our previous nomenclature (7).

Evidence to support the concept that activated metabolites of II are important for carcinogenesis has been presented (8-10). These studies have shown that NADPH-dependent mixed-function oxidases in liver microsomes produce reactive intermediates (epoxides) which can bind covalently to nucleic acids and proteins. Further studies have shown that epoxides are cleaved by a second microsomal enzyme, epoxide hydratase, to form dihydrodiols (11). The dihydrodiols are substrates for aryl hydrocarbon hydroxylase, which then generates diol-epoxides. It is the diol-epoxides of selected polycyclic aromatic hydrocarbon carcinogens that are thought to be the ultimate carcinogenic metabolites, binding to macromolecules to initiate tumor formation. Specific diol-epoxides of II such

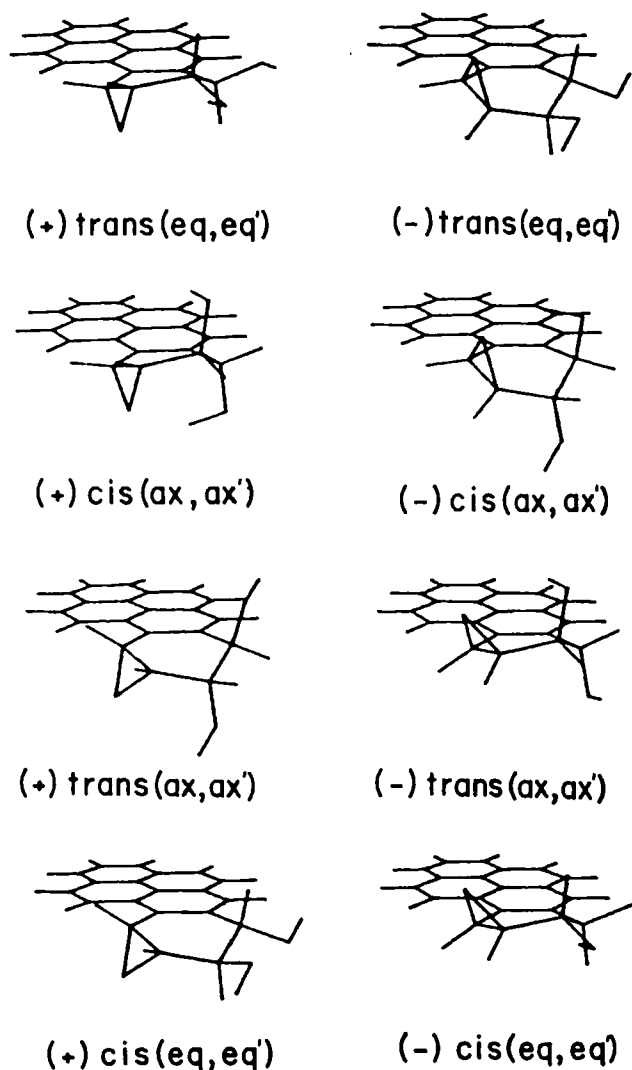
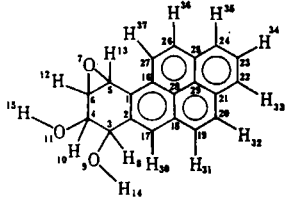


Figure 1—Computer-drawn representations of the structure-optimized geometries of the eight enantiomeric isomers of I.

as (+)-7β,8α-dihydroxy-9α,10α-epoxy-7,8,9,10-tetrahydrobenzo[a]pyrene have been shown to be potent inducers of neoplasia in mouse skin (12, 13). This pattern of metabolic reaction has been shown to occur in the skin and in cultured keratinocytes (14).

There is also considerable evidence that III residues bind covalently to both RNA (6) and DNA (15) predominantly at the 2-amino group of guanine. Cytosine and adenosine residues in nucleic acids are also alkylation targets to a

Table I—Optimized Molecular Parameters of the Four Isomers of I



Bond	Isomer			
	<i>cis</i> (ax,ax')	<i>trans</i> (eq,eq')	<i>trans</i> (ax,ax')	<i>cis</i> (eq,eq')
Bond Distance, Å				
C(1)—C(2)	1.412	1.412	1.411	1.412
C(2)—C(3)	1.477	1.471	1.472	1.470
C(3)—C(4)	1.487	1.485	1.485	1.484
C(1)—C(5)	1.457	1.456	1.459	1.457
C(5)—C(6)	1.453	1.452	1.452	1.451
C(6)—O(7)	1.406	1.405	1.406	1.405
C(3)—O(9)	1.394	1.386	1.389	1.386
C(4)—O(11)	1.387	1.387	1.385	1.387
C(3)—H(8)	1.131	1.136	1.132	1.137
C(4)—H(10)	1.134	1.133	1.132	1.132
C(6)—H(12)	1.122	1.122	1.122	1.123
C(5)—H(13)	1.121	1.121	1.123	1.123
O(9)—H(14)	1.043	1.034	1.033	1.034
O(11)—H(15)	1.033	1.033	1.032	1.033
C(1)—C(16)				
Bond Angle, °				
C(1)—C(2)—C(3)	120.2	120.3	120.7	120.6
C(2)—C(3)—C(4)	115.8	116.3	116.0	116.5
C(2)—C(1)—C(5)	118.1	119.1	118.4	118.8
C(1)—C(5)—C(6)	118.7	118.0	119.2	118.8
C(5)—C(6)—97	59.0	59.0	58.9	59.0
C(2)—C(3)—H(8)	111.3	105.3	110.4	104.5
C(2)—C(3)—O(9)	106.1	114.6	108.6	114.9
C(3)—C(4)—H(10)	108.5	108.6	108.9	109.1
C(3)—C(4)—O(11)	109.6	107.4	107.6	107.1
C(5)—C(6)—H(12)	119.0	118.9	119.2	119.1
C(6)—C(5)—H(13)	116.4	117.1	118.2	118.4
C(3)—O(9)—H(14)	102.8	107.9	107.2	108.0
C(4)—O(11)—H(15)	107.6	107.6	107.4	107.8
C(2)—C(1)—C(16)				
Dihedral Angle, °				
C(1)—C(2)—C(3)—C(4)	-31.7	-29.0	28.7	28.2
C(2)—C(1)—C(5)—C(6)	18.0	17.5	-13.0	-13.7
C(1)—C(5)—C(6)—O(7)	-106.2	-108.1	-108.7	-109.7
C(1)—C(2)—C(3)—H(8)	-159.1	88.9	153.0	-89.6
C(1)—C(2)—C(3)—O(9)	86.0	-154.2	-90.5	153.7
C(2)—C(3)—C(4)—H(10)	163.1	-80.8	-162.6	80.8
C(2)—C(3)—C(4)—O(11)	-79.4	162.6	81.5	-163.2
O(7)—C(6)—C(5)—H(12)	-100.6	-100.0	-99.0	-98.5
O(7)—C(6)—C(5)—H(13)	99.1	99.3	99.4	99.0
C(4)—C(3)—O(9)—H(14)	57.5	179.4	180.1	180.4
C(3)—C(4)—O(11)—H(15)	180.3	179.4	180.7	181.0

smaller extent, both *in vitro* (15–17) and *in vivo* (15, 18). The three bases contain an exocyclic amino group which presumably is the common alkylation site. This is relatively unusual since alkylation usually occurs at the N(7) position of guanine (19).

It has been reported (20) that 60–80% of the total adduct formed by (±)III with DNA involves the (+) enantiomer with the 2-amino group of *d*-guanine residues. A minor adduct is formed from the reaction of the (–) enantiomer with DNA. This minor adduct is present in greater amounts in denatured DNA than in native DNA. Small amounts of III-*d*-adenosine and III-*d*-cytosine adducts are also detected for both single- and double-stranded DNA. No differences in the total extent of (±)III binding to double- and single-stranded calf thymus DNA have been detected. It is thus of interest to identify I-DNA

Table II—Relative Energy and Net-Charge Distribution of the Four Isomers of I^a

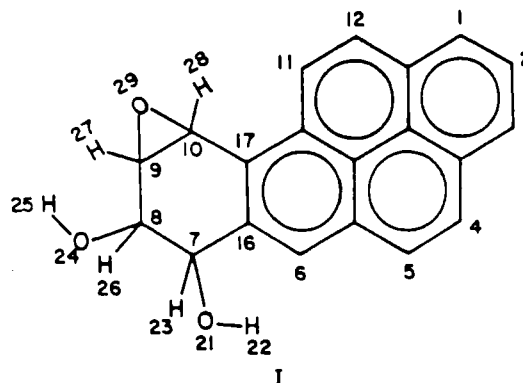
Atom	Isomer			
	<i>cis</i> (ax,ax')	<i>trans</i> (eq,eq')	<i>trans</i> (ax,ax')	<i>cis</i> (eq,eq')
Relative Energy, kcal/mole				
	0.00	1.20	4.48	4.64
Net-Charge, AMU				
C(1)	-0.011	-0.010	-0.007	-0.024
C(2)	0.006	0.001	0.004	0.003
C(3)	0.155	0.165	0.161	0.164
C(4)	0.143	0.155	0.153	0.149
C(5)	0.129	0.125	0.129	0.123
C(6)	0.104	0.098	0.095	-0.093
O(7)	-0.229	-0.221	-0.218	-0.219
H(8)	-0.023	-0.022	-0.038	-0.033
O(9)	-0.274	-0.253	-0.250	-0.250
H(10)	-0.031	-0.035	-0.033	-0.021
O(11)	-0.249	-0.239	-0.244	-0.242
H(12)	-0.015	-0.016	-0.017	-0.012
H(13)	-0.014	-0.015	-0.020	-0.019
H(14)	0.162	0.126	0.125	0.126
H(15)	0.124	0.122	0.131	0.124
C(16)	0.034	0.033	0.038	0.033
C(17)	-0.018	-0.021	-0.022	-0.020
C(18)	0.031	0.032	0.033	0.040
C(19)	-0.009	-0.010	-0.011	-0.011
C(20)	-0.008	-0.007	-0.006	-0.003
C(21)	0.033	0.032	0.032	0.031
C(22)	-0.011	-0.011	-0.011	-0.006
C(23)	0.005	0.005	0.004	0.005
C(24)	-0.011	-0.011	-0.011	-0.006
C(25)	0.032	0.032	0.032	0.031
C(26)	-0.006	-0.006	-0.006	0.002
C(27)	-0.013	-0.013	-0.011	-0.018
C(28)	0.011	0.009	0.011	0.003
C(29)	0.013	0.014	0.015	0.012
H(30)	-0.005	-0.009	-0.008	-0.009
H(31)	-0.007	-0.008	-0.008	-0.008
H(32)	-0.008	-0.007	-0.008	-0.007
H(33)	-0.007	-0.007	-0.007	-0.007
H(34)	-0.009	-0.008	-0.008	-0.009
H(35)	-0.008	-0.007	-0.007	-0.007
H(36)	-0.008	-0.007	-0.007	-0.007
H(37)	-0.008	-0.006	-0.004	-0.003

^a Using the numbering scheme presented in Table I.

stereochemical reaction models that are consistent with these experimental observations. Such theoretical models are essential for working hypotheses to explain the chemical reactivity of these carcinogenic species and, perhaps, their relative tumor induction potencies.

EXPERIMENTAL

The electronic structure of four isomers of I have been investigated and previously reported (7). In this study several approximations were employed for the estimation of the molecular structures of isomers of I. The substructure of the epoxy group was assumed to be the same as that of ethylene oxide. The local conformation of the two hydroxyl groups was fixed at that of ethylene glycol. Moreover, the "L" version (21) of the



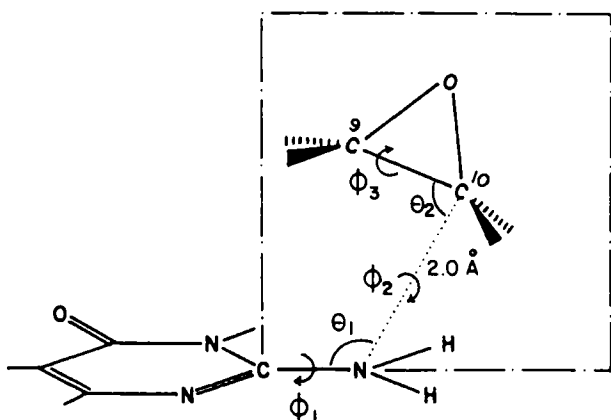


Figure 2—Transition-state geometry used to perform the steric reaction calculations. In the specific I-NH₃ transition-state geometry (7) used as the starting point in these calculations, $\phi_1 = 100^\circ$, $\theta_1 = 110^\circ$, $\phi_2 = 90^\circ$, $\theta_2 = 80^\circ$, and $\phi_3 = 0$ or 180° .

semiempirical CNDO/2 method was employed in which only π -electrons were explicitly taken into account for the conjugated subsystem.

In the present study, the conjugated part of the molecule was fixed at the idealized structure (C—C = 1.40 Å, C—H = 1.10 Å, angles = 120°). All other structural parameters were optimized using the CNDO/2 method. The optimized molecular parameters for each isomer are reported in Table I. Computer-drawn representations of the structure-optimized geometries of the eight enantiomeric isomers are shown in Fig. 1. The charge distributions and total energies for the structure-optimized molecules are reported in Table II. As found in the previous study (7), the *trans*(eq,eq') isomer (III) is more stable than the *trans*(ax,ax') isomer, and the *cis*(ax,ax') isomer (IV) is more stable than the *cis*(eq,eq') isomer. The angle between the epoxy group and the conjugated hydrocarbon ring system is larger in the more stable *trans* and *cis* isomers than in the corresponding less stable isomers. The longer C(3)—O(9) and O(9)—H(14) bond lengths (Table I) for IV are due to hydrogen bonding between the hydroxyl group and the epoxy oxygen. These results are consistent with those obtained in our previous study (7), although small differences in valence geometry exist.

In the previous study (7), the reactivity of the four isomers of I with the simple nucleophile ammonia was modeled. Isomer IV was found to

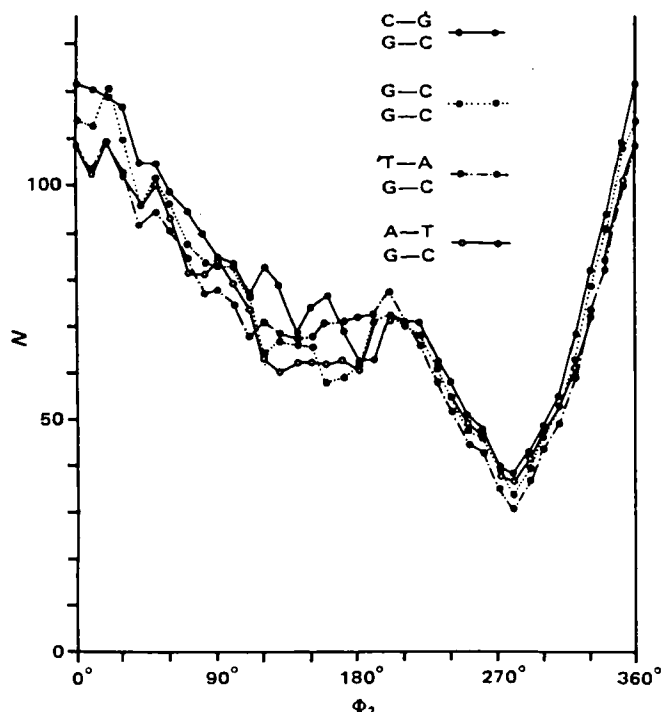


Figure 3—The least number of bad-contact interactions as a function of the transition-state geometry variable ϕ_2 for (+)III interacting with four sequences of B form DNA.

Table III—Least Number of Bad-Contacts at Three Nucleophilic Sites in Four Base-Pair Sequences Using (+)III

Site	Base-Pair Sequence			
	$\begin{array}{c} \uparrow \\ \text{C-G} \\ \downarrow \\ \text{G-C} \\ \uparrow \\ \text{C-G} \end{array}$	$\begin{array}{c} \uparrow \\ \text{G-C} \\ \uparrow \\ \text{G-C} \end{array}$	$\begin{array}{c} \uparrow \\ \text{T-A} \\ \downarrow \\ \text{G-C} \\ \uparrow \\ \text{T-A} \end{array}$	$\begin{array}{c} \uparrow \\ \text{A-T} \\ \downarrow \\ \text{G-C} \\ \uparrow \\ \text{A-T} \end{array}$
N(7)	8	9	10	11
O(6)	9	10	8	14
2-NH ₂	34	38	31	37

be the most reactive. These calculations allowed the identification of a unique transition-state geometry for alkylation. The transition state of I with ammonia corresponds to $\phi_1 = 100^\circ$, $\theta_1 = 110^\circ$, $\phi_2 = 90^\circ$, $\theta_2 = 80^\circ$, $\phi_3 = 0$ or 180° , and $r = 2.0$ Å (Fig. 2).

The calculations involving I and ammonia indicated that III and IV are both more stable, and also more reactive with the nucleophile, than the respective isomer complements, *trans*(ax,ax') and *cis*(eq,eq'). This may explain why III is observed to be the major metabolic isomer relative to *trans*(ax,ax'). Unfortunately, corresponding experimental studies of isomers of I with ammonia are not reported in the literature. The current studies have focused on (\pm)III and (\pm)IV, since biochemical observations have clearly indicated their particular importance.

The large size of I would be expected to impose steric constraints regarding its capacity to alkylate DNA. These steric constraints may limit the ways in which a transition-state geometry may be realized between an enantiomeric isomer of I and the exocyclic amino group of guanine in DNA. Therefore, it is necessary to examine intermolecular reaction geometries for the I-DNA complex. To do this it was assumed that the transition-state geometry for I-NH₂-guanine is the same as that found for the complex of I and ammonia (7). The "bad-contacts" between pairs of atoms from I and DNA were sought for the transition-state geometry shown in Fig. 2.

A bad-contact is assigned to an atom pair if the distance is shorter than a critical distance. If a specific conformation has one or more bad-contacts, it is assumed to have a high energy and cannot be realized. The critical distance, r_c , was selected to be the van der Waals distance for all interactions involving atoms of the aromatic rings of I. Smaller values than the corresponding van der Waals distances were chosen for interactions involving epoxide, diol, and saturated ring atoms (including hy-

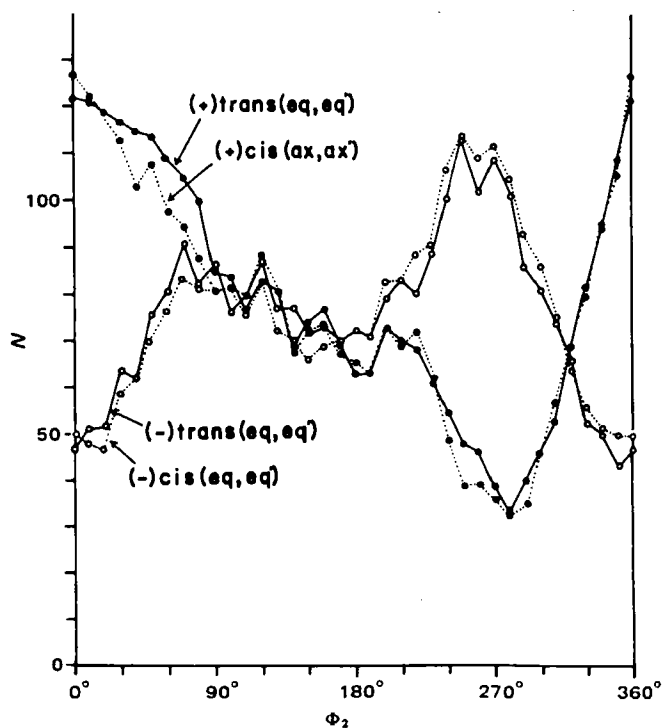
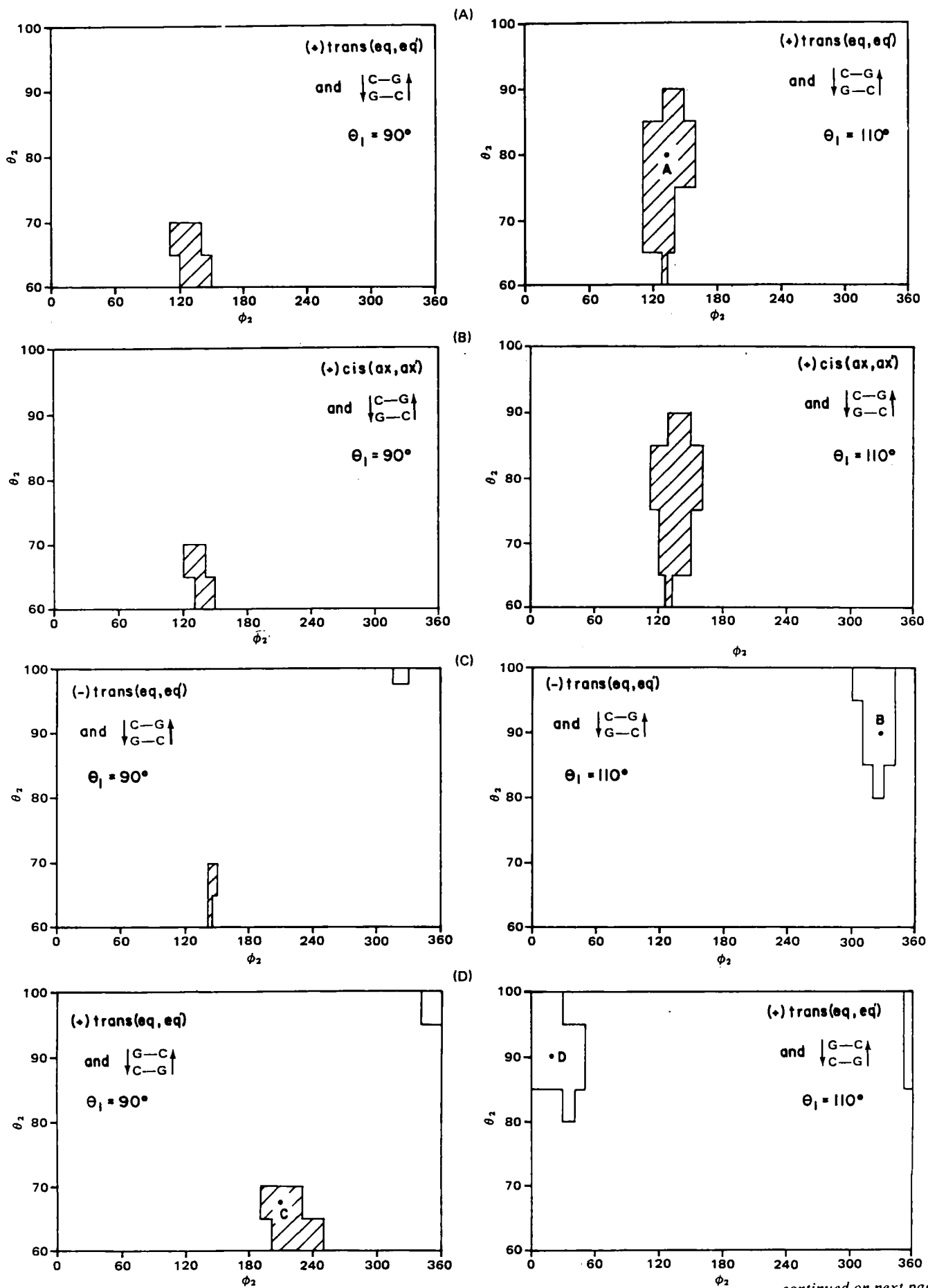


Figure 4—Plot of N versus ϕ_2 with the sequence of the interior two base pairs of the B form structure fixed at $\begin{array}{c} \uparrow \\ \text{C-G} \\ \downarrow \\ \text{G-C} \end{array}$.



continued on next page

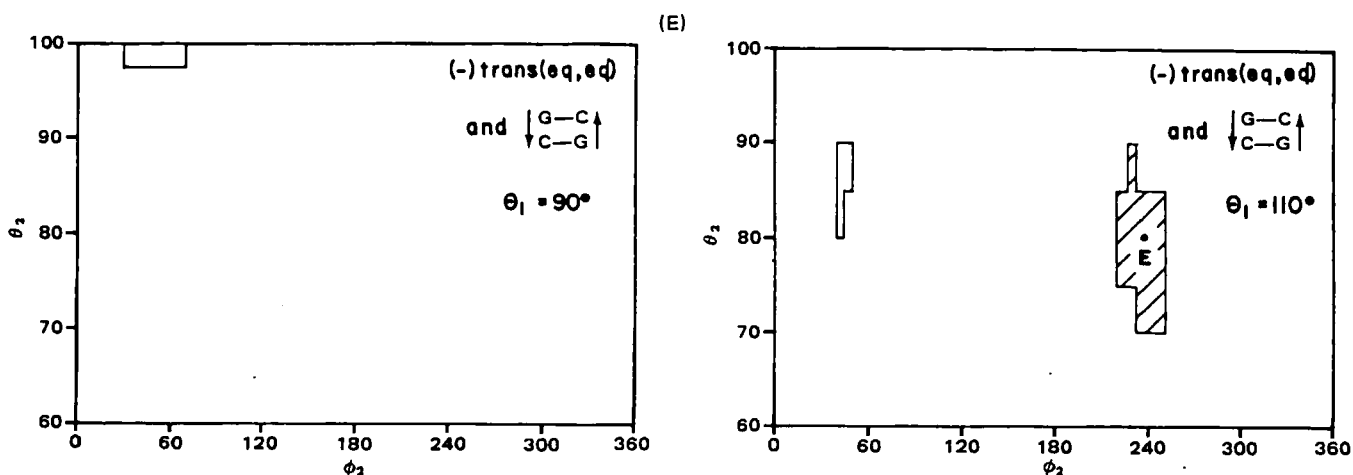


Figure 5—Steric contact plots of θ_2 versus ϕ_2 for different sequences of unwound dinucleoside dimer, (\pm)III, (\pm)IV, and two different values of θ_1 . The shaded regions correspond to allowed intercalation transition-state geometries. The open regions identify transition-state geometries in which I is outside the dinucleoside dimer. The letters A through E on the steric contact maps define the (ϕ_2, θ_2) values used to construct the stereo model figures in Fig. 7. The criteria for constructing the steric boundaries are given in Experimental.

Table IV—Atomic Coordinates of the Deformed DNA Structure and Intercalated (+)III

DNA											
C	1	3	-2.6680	8.7040	-3.3510	0.2400	2	3	4	25	0
H	2	1	-1.8640	9.4160	-3.5410	0.0520	1	0	0	0	0
H	3	1	-3.5880	9.2500	-3.5570	0.0520	1	0	0	0	0
H	4	3	-2.6420	7.4200	-4.1770	-0.0410	1	5	6	7	0
H	5	1	-2.2500	7.5660	-5.1830	0.0420	4	0	0	0	0
H	6	1	-3.6440	7.0040	-4.2670	0.0420	4	0	0	0	0
H	7	3	-1.6800	6.5480	-3.3770	0.1140	7	8	9	24	0
H	8	1	-0.6840	6.6760	-3.6010	0.0540	4	0	0	0	0
H	9	4	-2.0400	5.1620	-3.3770	-0.1030	7	10	22	0	0
H	10	2	-1.0453	4.1577	-3.3790	-0.2210	11	20	9	0	0
H	11	4	0.2858	4.4269	-3.3790	-0.3730	12	10	0	0	0
H	12	2	1.0219	3.3203	-3.3790	-0.4000	15	13	11	0	0
H	13	4	2.3602	3.3928	-3.3790	-0.2540	12	14	15	0	0
H	14	1	2.8498	4.3550	-3.3790	-0.1230	13	0	0	0	0
H	15	1	2.9484	2.4882	-3.3790	-0.1390	13	0	0	0	0
H	16	4	0.4840	2.0518	-3.3790	-0.2100	18	17	12	0	0
H	17	1	1.1349	1.1911	-3.3790	-0.1230	16	0	0	0	0
H	18	2	-0.6536	1.7512	-3.3790	-0.3550	16	19	20	0	0
H	19	7	-1.2530	0.5756	-3.3790	-0.3790	18	0	0	0	0
H	20	2	-1.6724	0.9297	-3.3790	-0.0950	18	10	21	0	0
H	21	4	-3.0518	3.0870	-3.3790	-0.1720	20	22	0	0	0
H	22	2	-3.2188	4.3838	-3.3790	-0.1190	21	23	9	0	0
H	23	1	-4.1651	4.9016	-3.3790	-0.0230	22	0	0	0	0
H	24	6	-1.6740	6.9380	-1.9130	-0.2710	7	25	0	0	0
H	25	3	-2.5420	8.1860	-1.6190	0.0940	1	24	26	27	0
H	26	1	-2.0420	9.9340	-1.3010	0.0510	25	0	0	0	0
H	27	3	-3.8400	7.7960	-1.2430	0.2090	25	28	29	30	0
H	28	1	-4.6720	8.2860	-1.7470	0.0530	27	0	0	0	0
H	29	1	-3.7720	9.2360	-0.2490	0.0530	27	0	0	0	0
H	30	6	-4.0580	9.3800	-1.3730	-0.3500	27	31	0	0	0
H	31	10	-5.1480	5.6720	-0.4410	-0.1640	30	32	34	35	0
H	32	7	-6.2780	6.4620	-0.3630	-0.5220	31	33	0	0	0
H	33	20	-9.3360	7.4140	-0.6910	0.0000	32	0	0	0	0
H	34	7	-5.3520	4.3240	-0.8770	-0.5220	31	0	0	0	0
H	35	6	-4.4020	5.6720	0.09730	-0.3500	31	36	0	0	0
H	36	3	-4.0900	4.4300	1.5890	0.2400	35	37	38	59	0
H	37	1	-4.3440	3.6160	0.0130	-0.0520	36	0	0	0	0
H	38	3	-2.6200	4.4280	2.0070	-0.0410	36	39	40	41	0
H	39	1	-2.1680	5.4160	2.0670	0.0420	38	0	0	0	0
H	40	1	-2.0380	3.8560	1.2876	0.0420	38	0	0	0	0
H	41	3	-2.6840	3.7700	3.3810	0.1140	38	42	58	43	0
H	42	1	-2.0680	4.3320	4.0810	-0.0540	41	0	0	0	0
H	43	4	-2.2700	2.3380	3.3770	-0.1750	41	44	53	0	0
H	44	2	-0.9623	1.8769	3.3770	-0.4220	43	45	46	0	0
H	45	7	-0.0403	2.7059	3.3770	-0.4190	44	0	0	0	0
H	46	4	-0.7378	0.5375	3.3770	-0.3440	44	47	0	0	0
H	47	2	-1.7635	-0.3234	3.3770	-0.3240	46	48	51	0	0
H	48	4	-1.4960	-1.6148	3.3770	-0.2220	47	49	50	0	0
H	49	1	-2.3038	-2.3320	3.3770	0.1170	48	0	0	0	0
H	50	1	-0.4699	-1.9539	3.3770	0.1300	48	0	0	0	0

continued

Table IV—continued

		DNA									
C	51	2	-3.1186	0.1269	3.3770	-0.1630	47	52	53	0	0
C	52	1	-3.9645	-0.5454	3.3770	-0.0200	51	0	0	0	0
C	53	2	-3.3193	1.4717	3.3770	-0.1900	51	54	43	0	0
C	54	1	-4.3310	1.8492	3.3770	-0.0030	53	55	56	57	0
N	55	20	1.5576	-1.6042	3.3770	0.0000	54	0	0	0	0
N	56	20	1.5576	-1.6042	3.3770	0.0000	54	0	0	0	0
N	57	20	1.5576	-1.6042	3.3770	0.0000	54	0	0	0	0
C	58	6	-4.1140	3.6860	3.8230	-0.2710	41	59	0	0	0
C	59	3	-4.7740	4.2800	2.9470	0.0940	58	36	60	61	0
C	60	1	-4.8460	5.2560	3.4290	0.0510	59	0	0	0	0
H	61	1	-5.7740	3.8680	2.8090	0.0510	59	62	0	0	0
N	62	20	0.0000	0.0000	-3.3770	0.0000	61	63	0	0	0
N	63	20	0.0000	0.0000	-3.3770	0.0000	62	64	0	0	0
C	64	3	9.7260	-0.6300	3.3570	0.2400	63	65	66	67	88
C	65	1	10.1880	-0.3380	3.5470	0.0520	64	0	0	0	0
C	66	1	10.8460	-1.3640	3.5630	-0.0520	64	0	0	0	0
C	67	3	8.4860	-0.9600	4.1830	-0.0410	64	68	69	70	0
C	68	1	8.5180	-0.5420	5.1870	0.0420	67	0	0	0	0
C	69	1	8.3660	-2.0380	4.2930	0.0420	67	0	0	0	0
C	70	3	7.3200	-0.2780	3.3830	0.1140	67	71	87	72	0
C	71	1	7.2240	0.7140	3.8070	-0.0540	70	0	0	0	0
C	72	4	6.9562	-1.0240	3.3830	-0.1030	70	73	85	0	0
C	73	2	4.9562	-0.2523	3.3850	-0.2210	74	83	72	0	0
C	74	4	3.3693	1.1056	3.3850	-0.3730	75	73	0	0	0
C	75	2	3.6993	1.5902	3.3850	-0.4000	79	76	74	0	0
C	76	4	3.4861	2.9134	3.3850	-0.2540	75	77	78	0	0
H	77	1	4.3226	3.5960	3.3850	-0.1230	76	0	0	0	0
H	78	1	4.4774	3.2963	3.3850	-0.1390	76	0	0	0	0
H	79	4	2.5737	0.7954	3.3850	-0.2100	81	80	75	0	0
H	80	1	1.5946	1.2489	3.3850	-0.1230	79	0	0	0	0
C	81	2	1.5702	-0.6049	3.3850	-0.3550	79	82	83	0	0
C	82	7	1.5007	-1.2151	3.3850	-0.3790	81	0	0	0	0
C	83	2	4.8892	-1.1257	3.3850	-0.0950	81	73	84	0	0
C	84	4	4.3356	-2.4403	3.3850	-0.1720	83	85	0	0	0
C	85	2	5.3383	-2.3284	3.3850	-0.1190	84	86	72	0	0
C	86	1	5.3450	-3.1432	3.3850	-0.0230	85	0	0	0	0
C	87	6	7.7560	-0.1500	1.9210	-0.2710	88	70	0	0	0
C	88	3	9.1940	-0.6500	1.9270	-0.0940	89	64	87	90	0
C	89	1	9.7740	0.0360	1.3130	0.0510	88	0	0	0	0
C	90	3	9.1600	-2.0060	1.2510	0.2090	88	91	92	93	0
C	91	1	9.8800	-2.6700	1.7550	0.0530	90	0	0	0	0
C	92	1	9.5800	-1.8200	0.2570	-0.0530	90	0	0	0	0
C	93	6	7.8800	-2.6080	1.3790	-0.3500	90	94	0	0	0
C	94	10	7.5020	-3.8500	0.4470	0.1640	93	95	97	98	0
C	95	7	8.5720	-4.7160	0.3690	-0.5520	94	96	0	0	0
C	96	20	9.5020	-4.5060	0.8970	-0.0000	95	0	0	0	0
C	97	7	6.2640	-4.4180	0.8830	-0.5520	94	0	0	0	0
C	98	6	7.2980	-3.1320	-0.9670	-0.3500	94	99	0	0	0
C	99	3	6.0200	-3.1780	-1.5830	-0.2400	98	100	101	122	0
C	100	1	5.3060	-3.6460	-0.9070	0.0520	99	0	0	0	0
C	101	3	5.6120	-1.7680	-2.0030	-0.0410	49	102	103	104	0
C	102	1	6.4380	-1.0580	-2.0630	0.0420	101	0	0	0	0
C	103	1	4.9600	-1.3660	-1.2850	0.0420	101	0	0	0	0
C	104	3	5.0060	-2.0100	-3.3750	0.1140	105	106	101	121	0
C	105	1	5.3680	-1.2620	-4.0750	0.0540	104	0	0	0	0
C	106	4	3.5100	-2.0080	-3.3710	-0.1750	104	107	116	0	0
C	107	2	2.7385	-0.8558	-3.3710	-0.4220	106	108	109	0	0
C	108	7	3.3125	0.2432	-3.3710	-0.4190	107	0	0	0	0
C	109	4	1.3854	-0.9710	-3.3710	-0.3440	107	110	0	0	0
C	110	2	0.8062	-2.1784	-3.3710	-0.3240	109	111	114	0	0
C	111	4	-0.5111	-2.2401	-3.3710	-0.2220	110	112	113	0	0
C	112	1	-1.0053	-3.2007	-3.3710	0.1170	111	0	0	0	0
C	113	1	-1.0945	-1.3303	-3.3710	-0.1300	111	0	0	0	0
C	114	2	1.5790	-3.3792	-3.3710	-0.1630	110	115	116	0	0
C	115	1	1.1378	-4.3655	-3.3710	0.0200	114	0	0	0	0
C	116	2	2.9315	-3.2396	-3.3710	-0.1900	114	117	106	0	0
C	117	1	3.5484	-4.1258	-3.3710	-0.0030	116	118	119	120	0
N	118	20	-1.2594	0.7205	-3.3710	0.0000	117	0	0	0	0
N	119	20	-1.2594	0.7205	-3.3710	0.0000	117	0	0	0	0
N	120	20	-1.2594	0.7205	-3.3710	0.0000	117	0	0	0	0
C	121	6	5.3160	-3.4060	-3.8150	-0.2210	104	122	0	0	0
C	122	3	5.0640	-3.8760	-2.9390	0.0940	99	121	123	124	0
C	123	1	7.0200	-3.6740	-3.4210	0.0510	122	0	0	0	0
C	124	1	5.9440	-4.9520	-2.8010	0.0510	122	0	0	0	0
N	125	20	13.9341	14.3471	0.0000	0.0000	0	0	0	0	0
Intercalated (+)III											
C	126	6	5.0571	2.8294	0.1434	-0.2280	127	128	0	0	0
C	127	3	5.4544	3.2476	-1.0658	0.1120	126	128	129	137	0
C	128	3	4.0629	3.4498	-0.7643	0.1270	126	127	130	131	0

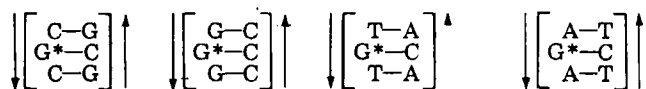
continued on next page

Table IV—continued

											Intercalated (+)III			
H	129	1	5.0113	3.9185	-1.7631	-0.0160	127	0	0	0				
H	130	1	3.4752	4.2843	-1.2126	-0.0110	128	0	0	0				
H	131	2	3.2975	2.2902	-0.3413	-0.0160	128	132	152	0				
H	132	2	3.9585	1.1315	0.0536	0.0080	131	133	141	0				
H	133	3	5.4160	1.0886	0.1013	0.1550	132	134	136	137				
H	134	6	5.8602	1.6040	1.3562	-0.2730	133	135	0	0				
*CH	135	1	5.5692	2.5245	1.4086	0.1620	134	0	0	0				
H	136	1	5.7342	0.0197	0.0031	-0.0190	133	0	0	0				
H	137	3	5.0105	1.6839	-0.9972	0.1340	127	133	138	140				
*CH	138	6	5.6951	1.2723	-2.7497	-0.2630	137	139	0	0				
H	139	1	6.1002	1.6147	-2.9428	0.1360	138	0	0	0				
H	140	1	7.1222	1.9261	-0.8684	-0.0280	137	0	0	0				
H	141	2	3.2206	0.0143	0.4915	-0.0150	132	142	155	0				
H	142	2	1.8208	0.0554	0.4745	0.0330	141	143	153	0				
H	143	2	1.0828	-1.0618	0.6824	-0.0080	142	144	156	0				
H	144	2	-0.3169	-1.0207	0.8654	-0.0090	143	145	157	0				
H	145	2	-0.9779	0.1380	0.4405	0.0330	144	146	154	0				
H	146	2	-2.3768	0.1795	0.4234	-0.0110	145	147	158	0				
H	147	2	-3.0378	1.3382	-0.0016	0.0060	146	148	159	0				
H	148	2	-2.2998	2.4553	-0.4094	-0.0120	147	149	160	0				
H	149	2	-0.9001	2.4143	-0.3925	0.0320	148	150	154	0				
H	150	2	-0.1621	3.5314	-0.8003	-0.0040	149	151	161	0				
H	151	2	1.2377	3.4904	-0.7834	-0.0190	150	152	162	0				
H	152	2	1.8986	2.3317	-0.3584	0.0210	131	151	153	0				
H	153	2	1.1598	1.2141	0.0496	0.0080	142	152	154	0				
H	154	2	-0.7391	1.2556	0.0325	0.0090	145	149	153	0				
H	155	1	3.7304	-0.8795	0.8193	-0.0020	141	0	0	0				
H	156	1	1.5927	-1.9556	1.2102	-0.0060	143	0	0	0				
H	157	1	-0.8862	-1.8825	1.1801	-0.0060	144	0	0	0				
H	158	1	-2.9461	-0.6823	0.7380	-0.0060	146	0	0	0				
H	159	1	-4.1170	1.3702	-0.0148	-0.0080	147	0	0	0				
H	160	1	-2.8097	3.3492	-0.7373	-0.0060	148	0	0	0				
H	161	1	-0.6720	4.4253	-1.1282	-0.0060	150	0	0	0				
H	162	1	1.8069	4.3522	-1.0980	-0.0040	151	0	0	0				

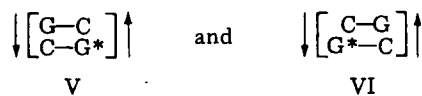
drogens) to qualitatively account for the uncertainty in molecular geometry and flexibility at the transition state. A set of r_c values that give a 5 kcal/mole repulsive energy in the 6–12 potential (22) for each unique atom pair was chosen subjectively in this work.

Four base-pair sequences of trinucleoside dimers in the B conformation (23) were considered:



The reaction of the central guanine (G^*) with (\pm)III and (\pm)IV was investigated. In each case the isomer was located "above" the central base pair, as shown in Fig. 2. In the first series of calculations, all conformational variables, except ϕ_2 , were held fixed. ϕ_2 was allowed to fully rotate in each case. For completeness, transition-state conformational analyses were also performed for the N(7) and O(6) positions on guanine. Transition-state geometries found in earlier studies (24) for these two sites were used as constraints in the analyses.

The transition-state I-NH₂-guanine conformational analyses were next repeated for two deformed dinucleoside dimer sequences:



The particular deformed conformation selected is that with the largest possible base-pair separation distance, $d = 6.76 \text{ \AA}$; it has been used previously in nucleic acid-drug intercalation studies (25). The atomic coordinates of this structure (along with (+)III intercalated between base pairs) are in Table IV. The nitrogen atom of the 2-amino group in the lower guanine, G^* , is attacked by the C(10) atom of I using the transition-state geometry shown in Fig. 2. Once again the conformational studies are characterized in terms of bad contacts. Since the N—C(10) distance is fixed at 2.0 \AA and $d = 6.76 \text{ \AA}$, the upper base pair has minimal influence on specifying bad contacts. The conformational degrees of freedom, defined in Fig. 2, were varied over the same range of values as used in the calculations for B form DNA.

RESULTS

The least number of bad contacts (N) was determined for each of the N(7), O(6), and 2-amino reactions with (\pm)III and (\pm)IV. As an example,

these least numbers are reported in Table III for (+)III [(+)trans(eq,eq') isomer]. Relative magnitudes in Table III may not be important. The essential observation is that in all cases bad contacts were found to exist. Figure 3 is a more detailed steric description of the 2-amino alkylation by (+)III. Nucleic acid sequence does not appear to alter the steric repulsions occurring in the transition state of the reaction. Figure 4 shows the dependence of N for 2-amino alkylation by (\pm)III and (\pm)IV as a function of transition-state conformation for *d*-(cytosine-guanine)₂. The steric effects in the 2-amino alkylation process by the (+) enantiomers are different from those of the (–) enantiomers. Nevertheless, alkylation by each form of I at the 2-amino position in guanine appears to be sterically unlikely from a study of Fig. 4. Alkylation at the N(7) or O(6) of guanine was also found to be sterically prohibited. It can be concluded from these conformational analyses that the B form of DNA cannot react with I because of steric hindrance for the selected transition-state geometries. Thus the experimental evidence (6, 8) which indicates 2-amino alkylation of guanine must be explained in terms of a deformation of the B form DNA structure. Of course, these results are dependent on the calculated transition-state geometry.

The two conformational degrees of freedom most critical to generating a stereochemically acceptable alkylation complex are θ_2 and ϕ_2 . Steric maps that define complexing geometries that are possible for the transition state are shown in Fig. 5. The shaded areas correspond to intermolecular geometries in which I is intercalated between base pairs. The other areas correspond to structures in which the I isomer is located outside the dinucleoside dimer. Several typical complex structures are shown in stereo-stick model representation in Fig. 6.

Both (+)III and (+)IV can react with the 2-amino group of guanine for V. Reaction with VI is more restricted for both these isomers. There is little difference in the steric constraints for (+)III and (+)IV alkylation to V. The results suggest that (+)trans(eq,eq') and (+)cis(ax,ax') alkylation with V should occur subsequent to intercalation.

There is no difference between the electronic structures of (+)III and (–)IV. However, experiments indicate that the (+) enantiomer alkylates guanine more efficiently than (–)III (20). Thus the intercalation and chemical reaction may be controlled by the absolute configurations of these enantiomers. Figures 5A and 5C indicate a large difference in the steric effect due to the enantiomeric properties of III. The (–) enantiomer is not expected to react with the 2-amino group of guanine in the V dimer through intercalation. However, for VI, different possible reaction geometries are predicted for (+) and (–)III (Figs. 5D and 5E). The (+) enantiomer is expected to intercalate and react with the 2-amino group

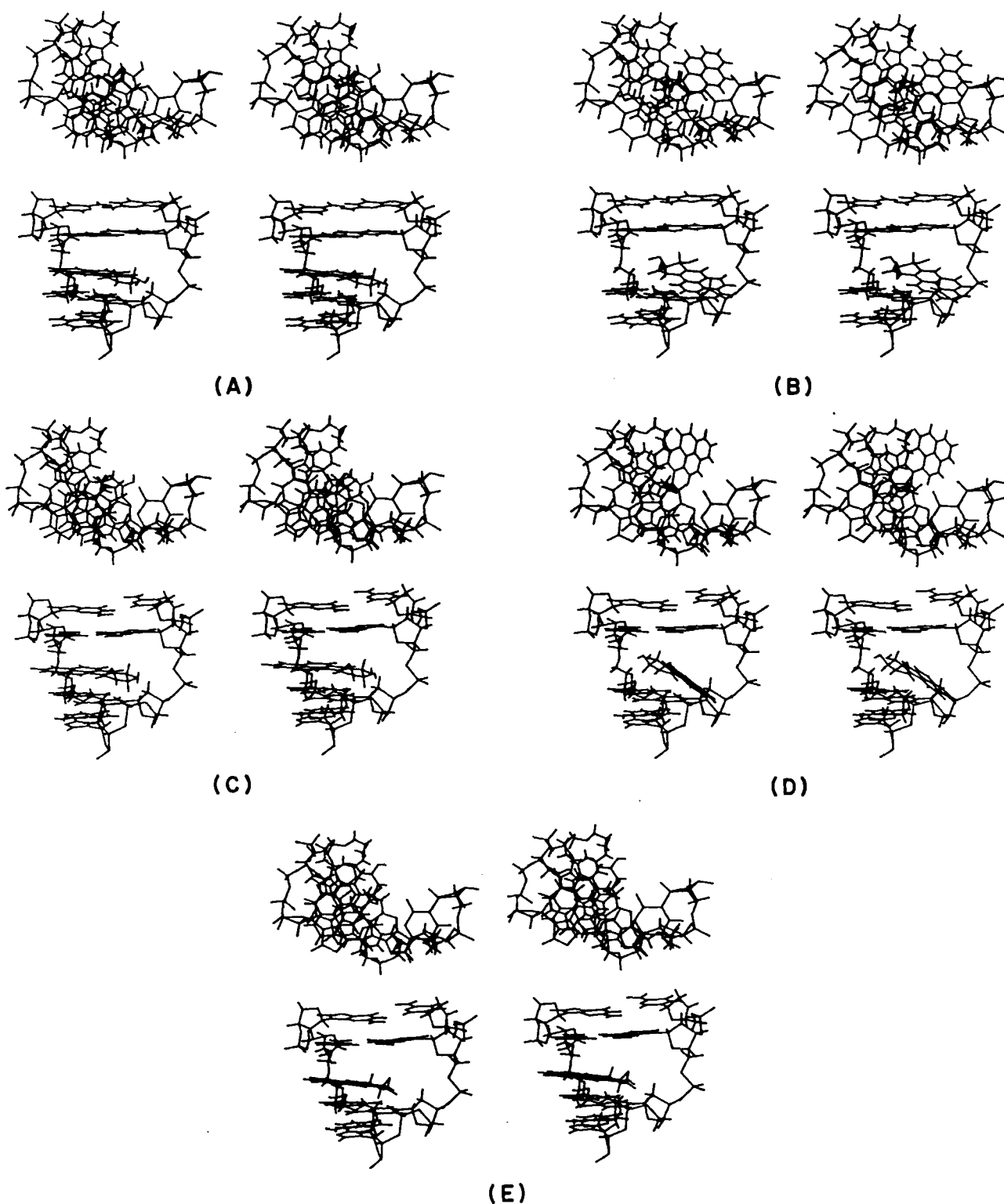


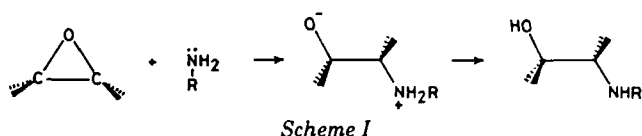
Figure 6—Stereo-stick models of sterically allowed I-dinucleoside dimer transition-state geometries defined in Fig. 6 (A–E on the steric contact maps). The top views are looking down the helix axis of the nucleic acid structure; the bottom figures are side views.

of guanine just above the nitrogen atom ($\theta_1 = 90^\circ$, Fig. 5D). The intercalated (–) enantiomer can reach the reaction site from slightly outside the dimer ($\theta_1 = 110^\circ$, Fig. 5C). Both the (+) and (–) enantiomers of III can react from outside the dimer helix. It is, however, not possible to deduce which reaction geometry is preferred since energetics are not included in the analysis.

The intercalation of isomers of I as a prerequisite for alkylation of the 2-amino of guanine is an interesting hypothesis. The intercalation process could be conceptualized as a physical catalyst which stabilizes the reaction geometry in a manner analogous to enzyme–substrate–inhibitor inter-

actions. However, the intercalation model requires that the I component of the reaction product remains between the base pairs. Experimental studies indicate, however, that the adduct involving I is located outside the DNA structure (26). The conformational analysis of the I open-form model of DNA indicates that the part of the reaction product involving I cannot come outside of the base pairs by rotation about the adduct C(10)–N bond unless the hydrogen bond involving the exocyclic amino group of guanine and the cytosine oxygen is broken.

Thus the change in the hydrogen bonding energy for such a reaction process (Scheme I) was examined, and the relative energies of the three



states of the G-C base pair (Fig. 7) were compared. The CNDO/2 method was used (27). The methyl group attached at the nitrogen atom was placed above the base-pair plane to fit the reaction product model with I held between base pairs. The results of these calculations suggest that if the hydrogen bond between the 2-amino group of guanine and the O of cytosine is broken during the alkylation process, allowing I to rotate out from between the base pairs, the resultant base-pairing structure could be of lower, or at least comparable, energy to that of the intercalation structure (Fig. 8).

DISCUSSION

Two major hypotheses were made in this study: (a) the transition-state geometries of isomers of I with the exocyclic amino group of guanine are identical to that calculated for isomers of I interacting with ammonia (7), and (b) the sterically allowed transition-state geometries of isomers of I with dinucleoside dimers can be identified using the aforementioned stereochemical model (*Experimental*).

The most clear-cut finding from the investigation is that neither (\pm)III or (\pm)IV can alkylate the 2-amino group of guanine for B form DNA. This reaction is stereochemically prohibited based on the postulated transition-state geometries. The deformation in the conformation of double-stranded DNA that is associated with this alkylation process has not been uniquely identified. However, if a dinucleoside dimer is unwound, so that the distance between base pairs is maximized ($d = 6.76 \text{ \AA}$), two possible geometric reaction models result. In one, alkylation occurs when I is located outside the nucleic acid structure; in the other, I is intercalated between base pairs for the alkylation transition state. Intercalation of I could serve as a physical catalyst, or provide at least substrate stabilization, for NH_2 -guanine alkylation. The alkylation transition-state geometry is sensitive to nucleic acid sequence for both the isomeric and enantiomeric forms of I.

The choice of the deformed structure of the double-stranded DNA model is somewhat arbitrary. However, the structure selection should correspond to that in which one strand exerts the least steric influence on the interaction between I and the other strand. This is an important consideration since the total extent of (\pm) binding to I to single- and double-stranded DNA is the same (20). Conversely, this observation also requires that the stereochemical constraints for NH_2 -guanine alkylation in double-stranded structures are no more severe than in the single-stranded DNA. This study has focused on double-stranded DNA because its local conformational properties are better understood, and because

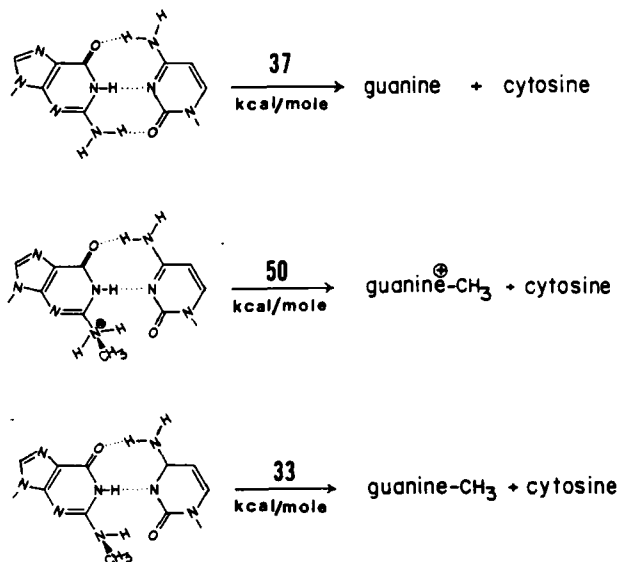


Figure 7—The G-C base-pair transition-state energies associated with breaking and restructuring the (guanine 2- NH_2)-(cytosine oxygen) base-pair hydrogen bond.

the double-stranded structure introduces more steric repulsive sites than a single strand.

The calculations reported here are based in part on "soft" steric contact distances (those atoms of the diols, epoxide, and saturated ring of I). As such, this model cannot be used to identify the preferred transition-state geometry. The following paper explores in detail the physical interaction of I with nucleic acid structures to better quantify allowed intermolecular geometries, with special emphasis on possible intercalation mechanisms.

REFERENCES

- (1) A. Borgen, H. Darvey, N. Castagnoli, T. T. Crocker, R. E. Rasmussen, and I. Y. Wang, *J. Med. Chem.*, **16**, 502 (1973).
- (2) P. Sims, P. L. Grover, A. Swaisland, K. Pal, and A. Hewer, *Nature (London)*, **252**, 326 (1974).
- (3) P. Daudel, M. Duquesne, P. Vigny, P. L. Grover, and P. Sims, *FEBS Lett.*, **57**, 250 (1975).
- (4) H. W. S. King, S. R. Osborne, F. A. Beland, R. G. Harvey, and P. Brookes, *Proc. Natl. Acad. Sci. USA*, **73**, 2679 (1976).
- (5) V. Ivanovic, N. E. Geacintov, and I. B. Weinstein, *Biochem. Biophys. Res. Commun.*, **70**, 1172 (1976).
- (6) I. B. Weinstein, A. M. Jeffrey, K. W. Jennette, S. H. Blobstein, R. G. Harvey, C. Harris, H. Atrup, H. Kasai, and K. Nakanishi, *Science*, **193**, 592 (1976).
- (7) O. Kikuchi, A. J. Hopfinger, and G. Klopman, *Cancer Biochem. Biophys.*, **4**, 1 (1979).
- (8) J. A. Miller and E. C. Miller, in "Environmental Carcinogenesis," P. P. Kimmellot and E. Kriek, Eds., Elsevier, Amsterdam, 1979, p. 228.
- (9) D. M. Jerina and J. W. Doly, *Science*, **185**, 573 (1974).
- (10) P. L. Grover and P. Sims, *Biochem. J.*, **110**, 154 (1968).
- (11) F. Olsch, *Ciba Found. Symp.*, **76**, 169 (1980).
- (12) T. J. Slaga, W. M. Bracken, A. Biaje, W. Levin, H. Yagi, D. M. Jerina, and A. H. Conney, *Cancer Res.*, **39**, 67 (1979).
- (13) M. Koreeda, P. D. Moore, P. G. Wislocki, W. Levin, A. H. Conney, H. Yagi, and D. M. Jerina, *Science*, **199**, 778 (1978).
- (14) E. K. Parkinson and R. F. Newbold, *Int. J. Cancer*, **26**, 289, 1980.
- (15) A. M. Jeffrey, K. W. Jennette, K. Gvzeskowiak, K. Nakanishi, R. G. Harvey, H. Atrup, and C. Harris, *Nature (London)*, **269**, 348 (1977).
- (16) T. Meehan and K. Straub, *ibid.*, **277**, 410 (1979).
- (17) A. M. Jeffrey, K. Gvzeskowiak, I. B. Weinstein, K. Nakanishi, P. Roller, and R. G. Harvey, *Science*, in press.
- (18) V. Ivanovic, N. E. Geacintov, H. Yamasaki, and I. B. Weinstein, *Biochemistry*, **17**, 1597 (1978).
- (19) P. D. Lawley, in "Chemical Carcinogens ACS Monograph 173," C. E. Searle, Ed., American Chemical Society, Washington, D.C., 1976, p. 83.
- (20) P. Pulkrabek, S. Leffler, D. Grunberger, and I. B. Weinstein, *Biochemistry*, **18**, 5128 (1979).
- (21) O. Kikuchi, A. J. Hopfinger, G. Klopman, *J. Theor. Biol.*, **77**, 129 (1979).
- (22) A. J. Hopfinger, "Conformational Properties of Macromolecules," Academic, New York, N.Y., 1973.
- (23) J. N. Davidson, "The Biochemistry of the Nucleic Acids," 8th ed., Academic, New York, N.Y., 1976, p. 94.
- (24) O. Kikuchi, A. J. Hopfinger, and G. Klopman, *Biopolymers*, **19**, 325 (1980).
- (25) Y. Nakata and A. J. Hopfinger, *Biochem. Biophys. Res. Commun.*, **95**, 583 (1980).
- (26) N. E. Geacintov, A. Gagliano, V. Ivanovic, and I. B. Weinstein, *Biochemistry*, **17**, 5256 (1978).
- (27) J. A. Pople and D. L. Beveridge, "Approximate Molecular Orbital Theory," McGraw-Hill, New York, N.Y., 1970.

ACKNOWLEDGMENTS

This work was supported by the National Cancer Institute (Contract N01-CP-65927), the National Institutes of Health (Grants ES-1900 and OH-1147), the Research Service of the Veterans Administration, and Adria Laboratories of Columbus, Ohio.

We appreciate the helpful discussions with D. Malhotra of our laboratory and Dr. S. Yang of the Uniformed Services University of the Health Sciences.